

# Crystallization of isotactic polypropylene/natural terpene resins blends

C. Silvestre\*, S. Cimmino, E. D'Alma, M.L. Di Lorenzo, E. Di Pace

*Istituto di Ricerca e Tecnologia delle Materie Plastiche IRTEMP-CNR, Via Toiano 6, 80072 Arco Felice (NA), Italy*

Received 3 February 1998; accepted 22 September 1998

## Abstract

The influence of two natural terpene resins on the morphology, phase structure and isothermal crystallization process of iPP was investigated by optical (OM) and electron microscopy (SEM) and differential scanning calorimetry (DSC). It was found that in dependence on temperature, composition and chemical nature of the resin, one, two or three phases can be present. The isothermal spherulite growth rate and overall crystallization rate of the blends are depressed compared to plain iPP. This depression was attributed to the increase of the energies relative to the transport of macromolecules in the melt and to the formation of nuclei of critical size, following the addition of resin. The presence of resin seems to lead to the formation of more regular folding surfaces. © 1999 Elsevier Science Ltd. All rights reserved.

*Keywords:* Isotactic polypropylene; Terpene resin; Blends

## 1. Introduction

Isotactic polypropylene (iPP) is a thermoplastic material widely used in several sectors, as it offers interesting combinations of good mechanical performance, heat resistance, fabrication flexibility and low cost.

In the food packaging sector the use of iPP, already conspicuous, is predicted to increase in the next years [1], even if this polymer is relatively permeable to oxygen compared to other plastic materials [see for example nylon, poly(vinyl chloride), poly(ethylene terephthalate), poly(ethylene-co-vinyl alcohol) and poly(vinylidene chloride)] [2]. Therefore several studies are oriented to decrease the diffusion of gases through the polymer walls. One of the approaches consists in the addition of a certain amount of a second component to the iPP. Few years ago, an iPP based film with reduced permeability to oxygen was obtained, adding a petroleum derived resin, the hydrogenated oligocyclopentadiene (HOCP), to iPP [3].

The commercial interest in this blend was comparable and related to the scientific one. In fact a phase diagram with a closed loop was obtained, on which basis, changing composition and temperature, different phase structures, morphologies and properties were obtained [4–6].

The HOCP could be successfully replaced by some terpene resins, obtained by oligomerization of exudates of trees

and plants, low value by-products of the wood processing industries. The polyterpenes are low molecular weight materials with a structure similar to that of hydrocarbon resins and are glassy at room temperature.

The aim of this paper is to analyze, as a function of composition, temperature and preparation conditions, the morphological and thermodynamic properties related to the isothermal crystallization from the melt of iPP/Poly( $\alpha$ -pinene) (iPP/P $\alpha$ P) and iPP/Poly(d-limonene) (iPP/PL) blends.

The main objective of such a study is to produce eco-sustainable food packaging materials through mixing the iPP with natural resins.

The mechanical and rheological properties, the permeability to gases of these blends will be the subjects of companion papers [7,8].

## 2. Experimental

### 2.1. Materials

Isotactic polypropylene (iPP) is a commercial product, Shell HY 6100, with  $M_w = 3.0 \times 10^5 \text{ g mol}^{-1}$ .

Poly( $\alpha$ -pinene) (P $\alpha$ P) and poly(d-limonene) (PL) are commercial resins kindly supplied by Hercules (The Netherlands).

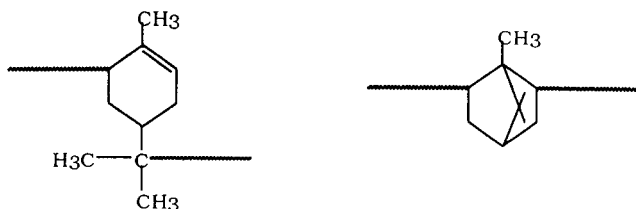
The P $\alpha$ P derives from the polymerization of  $\alpha$ -pinene monoterpene, the main constituent of the wood of coniferous plants. The sample used is the Piccolyte A115, with softening point (R&B) = 115°C,  $T_g = 61^\circ\text{C}$ ,  $M_n =$

\* Corresponding author. Tel.: + 39-081-8534174; fax: + 39-081-8663378.

E-mail address: silv@mail.irtemp.na.cnr.it (C. Silvestre)

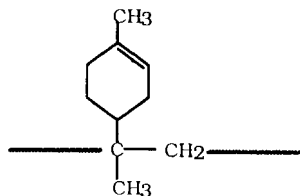
680 g mol<sup>-1</sup>,  $M_w = 1075$  g mol<sup>-1</sup> and  $M_z = 1650$  g mol<sup>-1</sup> (Hercules data).

The structure of P $\alpha$ P is not exactly known. Recently the following structures were proposed [9]:



The PL derives from the polymerization of d-limonene monoterpene that is the main constituent of the essential oil of citrus fruits, especially from the peels of oranges and lemons. The PL resin used is the Piccolyte C115 with softening point (R&B) = 115°C,  $T_g = 59^\circ\text{C}$ ,  $M_n = 625$  g mol<sup>-1</sup>,  $M_w = 1150$  g mol<sup>-1</sup> and  $M_z = 2050$  g mol<sup>-1</sup> (Hercules data).

The proposed structure of PL is [10]:



## 2.2. Blend preparation

iPP, P $\alpha$ P and PL components were mixed in a Brabender-like apparatus (Rheocord EC of HAAKE Inc.) at 210°C and 32 rpm for 10 min. The mixing ratios of iPP/resin (wt/wt) were: 100/0, 95/5, 90/10, 80/20, and 70/30.

Preliminary experiments performed by thermogravimetric analysis (TGA) have shown that the blend components do not undergo any thermal degradation during the mixing.

## 2.3. Preparation of compression-molded samples

The mixed material was compression-molded in a heated press at a temperature of 210°C for 5 min without any applied pressure to allow complete melting. After this period, a pressure of 100 bar was applied for 5 min. Then the plates of the press, containing coils for fluids, were rapidly cooled to room temperature by cold water in about 2 min. Finally the pressure was released and the mold removed from the plates. The mold had a parallelepiped shape (65 × 100 mm), and thickness of 1.0 mm.

## 2.4. Calorimetric measurements

The overall isothermal kinetics of crystallization of the blends were investigated with a differential scanning calorimeter (Mettler DSC-30). The samples (about 10–15 mg)

were heated from 25°C to 200°C, melted at 200°C for 10 min, then rapidly cooled to the desired  $T_c$  and allowed to crystallize.

The heat evolved during the isothermal crystallization was recorded as a function of time. The fraction  $X_t$  of the material crystallized after a period of time  $t$  was calculated by the relation:

$$X_t = \frac{\int_0^t \left( \frac{dH}{dt} \right) dt}{\int_0^\infty \left( \frac{dH}{dt} \right) dt}$$

where the first integral is the heat generated at time  $t$  and the second one is the total heat when the crystallization is complete. Plotting  $X_t$  against time, the half-time of crystallization,  $\tau_{1/2}$ , defined as the time taken for half of the crystallinity to develop, was obtained.

## 2.5. Optical microscopy

The morphology and the isothermal spherulite growth rate were studied by using a Zeiss Axioscop polarizing optical microscope, fitted with a Linkam TH600 hot stage.

The radial growth rate,  $G = dr/dt$  (where  $r$  is the radius of the spherulites and  $t$  the time), was calculated by measuring the size of iPP spherulites during the isothermal crystallization process. The standard procedure was the following: each sample was sandwiched between two microscope slides, heated at 200°C for 10 min, then rapidly cooled to  $T_c$  and allowed to crystallize. The radial growth rate of a spherulite focused upon was finally monitored during crystallization by taking photomicrographs at appropriate intervals of time. From the plots of  $r$  against the time,  $G$  was calculated as the slope of the resulting straight lines.

## 2.6. Scanning electron microscopy

The morphology of the blends was analyzed by electron microscopy, using a SEM 501 Philips microscope on cryogenically fractured surfaces of the samples. Before the electron microscopy observation, the surfaces were coated with Au–Pd alloy with a SEM coating device (SEM Coating Unit E5150-Polaron Equipment Ltd).

# 3. Results and discussion

## 3.1. Morphology and structure

Utilizing optical and electron microscopy it has been pointed out that the overall morphology and the phase structure depend on the temperature, crystallization conditions, composition and type of resin.

A series of optical and electron micrographs of iPP samples and of its blends with P $\alpha$ P and PL isothermally crystallized from the melt at  $T_c = 126^\circ\text{C}$  and  $130^\circ\text{C}$  is reported in Figs. 1–7.

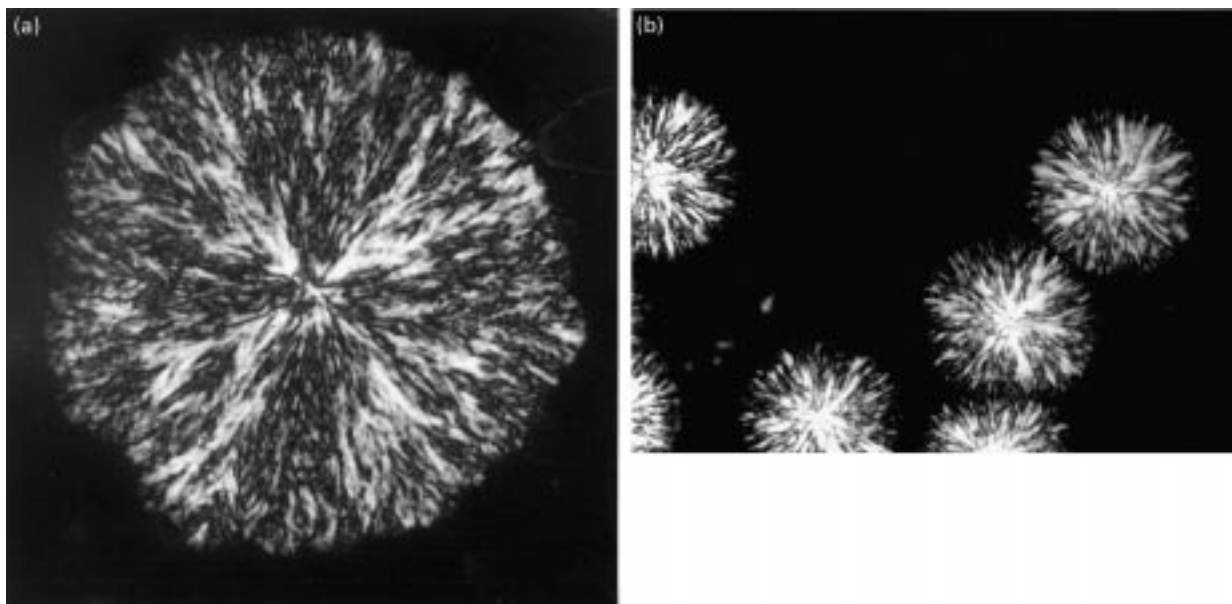


Fig. 1. Optical micrographs of iPP/resin 70/30 blends during the crystallization at  $T_c = 130^\circ\text{C}$ : (a) iPP/P $\alpha$ P; (b) iPP/PL (crossed polars).

For all the blends in the melt at  $200^\circ\text{C}$  no segregated domains in the matrix of iPP are observed, suggesting either miscibility between the components or that the dimension of domains of a possible dispersed phase is below the resolution obtainable by optical microscopy ( $2000 \text{ \AA}$ ).

Decreasing the temperature, the morphology remarkably changes. In fact at  $T_c$ , a liquid–solid phase separation due to the iPP crystallization takes place (see Fig. 1). Polypropylene crystals segregate forming a separate phase. The remaining amorphous phase is homogeneous by optical microscopy results. In fact, both during and at the end of the crystallization process, no segregate domains are visible, suggesting that the resin is probably present in the interlamellar and/or interfibrillar regions of spherulites (see Fig. 1).

In order to have information on the miscibility in the amorphous phase, the samples were examined using a scanning electron microscope (SEM).

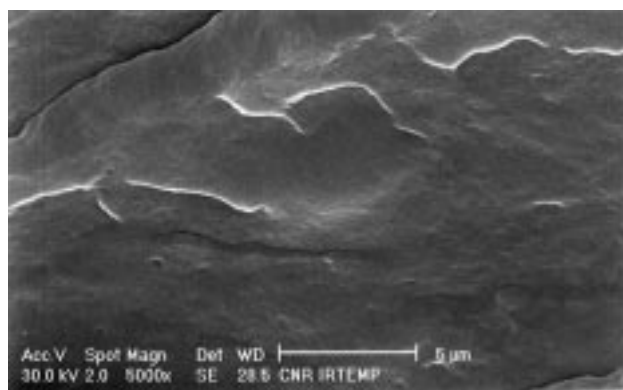


Fig. 2. Electron micrograph of fracture surface of isothermally crystallized sample of iPP at  $T_c = 126^\circ\text{C}$ .

Electron micrographs of fracture surfaces of isothermally crystallized samples at  $T_c = 126^\circ\text{C}$  are reported in Figs. 2–4 for pure polypropylene and for iPP/P $\alpha$ P and iPP/PL blends, respectively.

The iPP/P $\alpha$ P isothermally crystallized blends, for all the compositions analyzed, present fracture surfaces without evidence of segregated domains (see Fig. 3).

For iPP/PL blends the morphology depends on the composition. In fact, as it is possible to note in Fig. 4, for the iPP/PL 90/10 sample the fracture surface does not show domains of dispersed phase, whereas for iPP/PL 80/20 and 70/30 blends the fracture surfaces are characterized by the presence of segregated domains (see Fig. 4(b and c)).

Adding these morphological evidences to those obtained by optical microscopy, it results that:

1. All the iPP/P $\alpha$ P blends studied are homogeneous in the amorphous phase. After crystallization the iPP/P $\alpha$ P blends are therefore constituted of two phases: a crystalline phase of iPP and one homogeneous amorphous phase constituted by amorphous iPP and P $\alpha$ P. The morphological observations suggest that the P $\alpha$ P is enclosed in the interlamellar regions of the iPP crystals.
2. The iPP/PL 90/10 blend is homogeneous, whereas the iPP/PL 80/20 and 70/30 blends are characterized by two amorphous phases. These two phases are very likely conjugated, as preliminary results obtained by DSC and DMTA have indicated [8]. After crystallization, the 80/20 and 70/30 blends are constituted of three phases: a crystalline phase of iPP and two amorphous phases.

As already observed in the Fig. 1, the polypropylene crystallizes according to a spherulitic morphology. The spherulite dimensions depend on the crystallization temperature, composition and type of resin. For all the

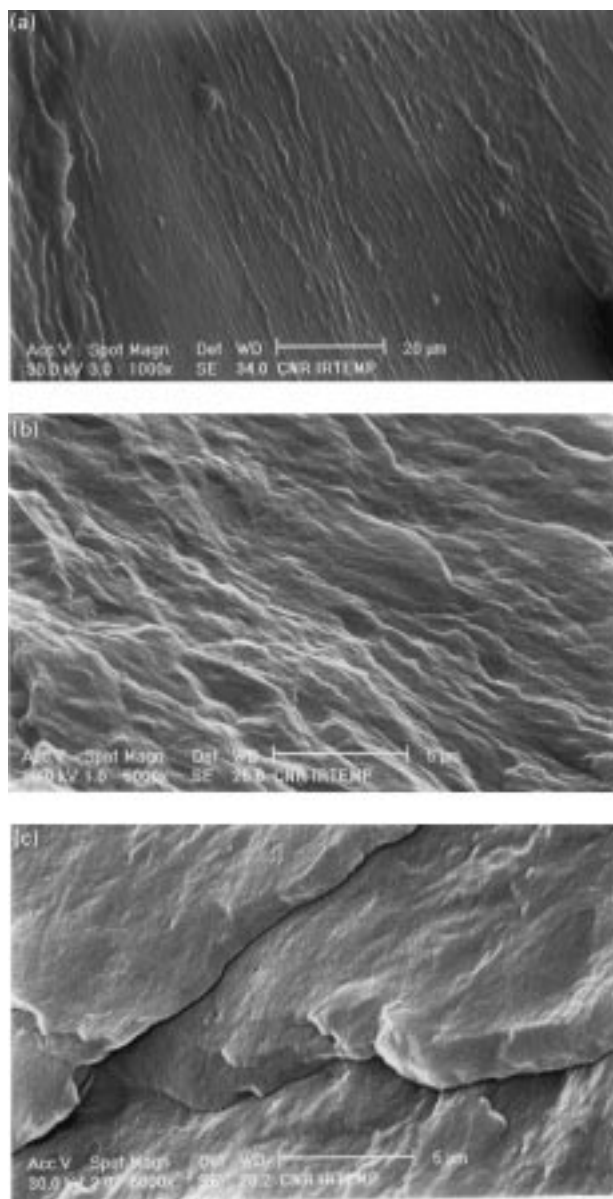


Fig. 3. Electron micrographs of fracture surfaces of isothermally crystallized samples of iPP/P $\alpha$ P blends at  $T_c = 126^\circ\text{C}$ : (a) 90/10; (b) 80/20; (c) 70/30.

samples, the number of spherulites for unit of area, ( $N$ ), decreases with increase in temperature, in agreement with the kinetic theory of crystallization [11], that predicts a decrease in the nucleation rate and density with  $T_c$ .

In the case of the iPP/P $\alpha$ P system, for a same  $T_c$ , the nucleation density always decreases with the increase of content of the resin in the blend (see Figs. 5 and 6). Such a decrease is probably produced by the dilution of the iPP nuclei as a result of the substitution of iPP with P $\alpha$ P.

For the iPP/PL system, the dependence of nucleation density on composition is more complex (see Fig. 7). Adding up to 20% of PL to iPP,  $N$  decreases in analogy to what happens for iPP/P $\alpha$ P blends (see Fig. 7(a and b)).

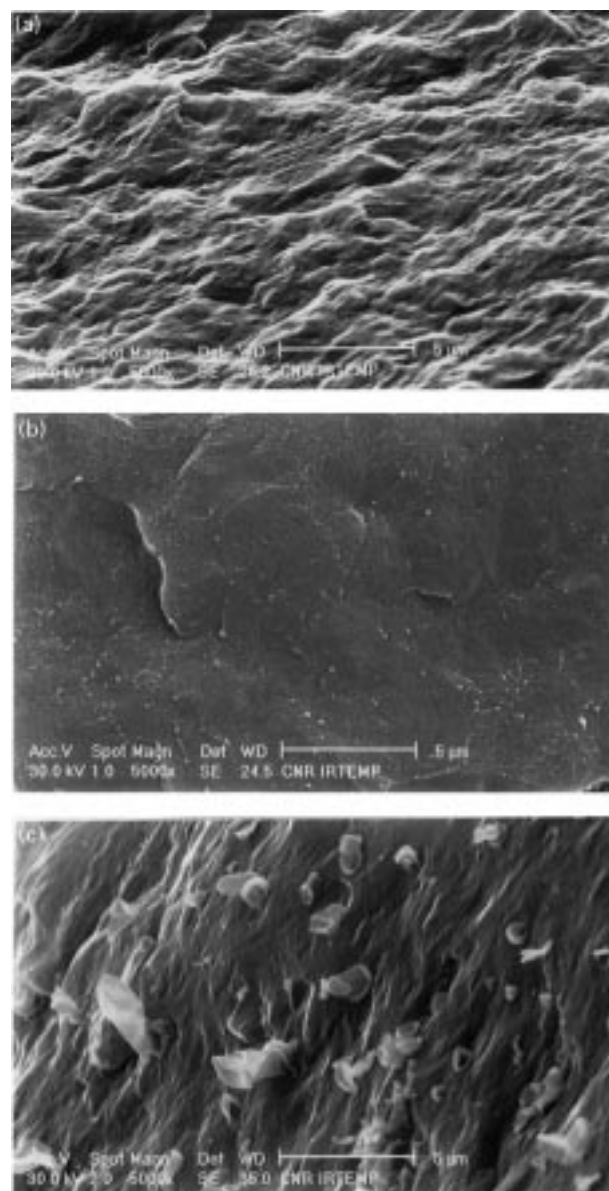


Fig. 4. Electron micrographs of fracture surfaces of isothermally crystallized samples of iPP/PL blends at  $T_c = 126^\circ\text{C}$ : (a) 90/10; (b) 80/20; (c) 70/30.

Adding 30% of poly(d-limonene) to iPP (see Fig. 7(c)) there is an unexpected increase in the  $N$  value, that, at a given  $T_c$ , approximately reaches that relative to pure polypropylene. Considering that for blends at higher content of PL a phase separation has been observed, this result suggests that the domains of the phase rich in resin can behave like nucleating agents and this effect balances and prevails over the dilution effect.

### 3.2. Crystallization process

#### 3.2.1. Spherulite radial growth

The spherulite radial growth rate ( $G$ ) as a function of temperature for a pure component can be expressed through

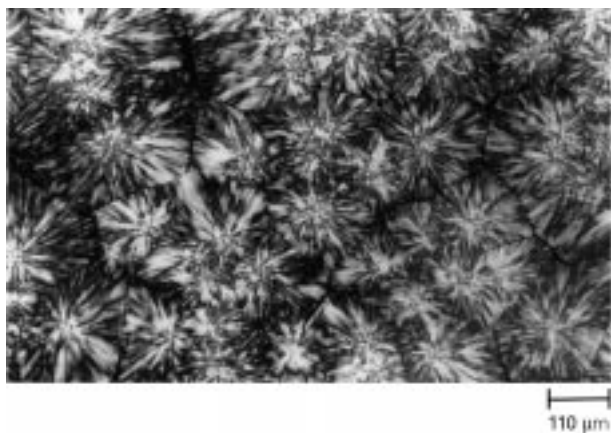


Fig. 5. Optical micrograph of isothermally crystallized sample of iPP at  $T_c = 130^\circ\text{C}$  (crossed polars).

the Hoffman and Lauritzen equation [12]:

$$\ln G + \frac{U^*}{R(T_c - T_\infty)} = \ln G_0 - \frac{K_g}{T_c \Delta T f} \quad (1)$$

where  $G_0$  is a pre-exponential term;  $R$  the universal gas constant;  $U^*$  the energy for the transport of the macromolecules in the melt;  $T_c$  the crystallization temperature;  $T_\infty$  the temperature where all the motions associated with the viscous flow stop, defined as  $(T_g - C)$  where  $C$  is a constant, that can assume different values;  $\Delta T$  the undercooling,  $(T_m^0 - T_c)$ ;  $f$  a corrective factor that takes into account the variation of the equilibrium melting enthalpy ( $\Delta H_m^0$ ) with temperature, defined as  $2T_c/(T_c + T_m^0)$ ;  $K_g$  a term connected with the energy required for the formation of nuclei of critical size, defined as  $nb\sigma\sigma_c T_m^0/\Delta H_m^0 k$ ; and  $n$  a variable that considers the crystallization regime and assumes the value 4 for the regime I and III, and the value 2 for the regime II [13].

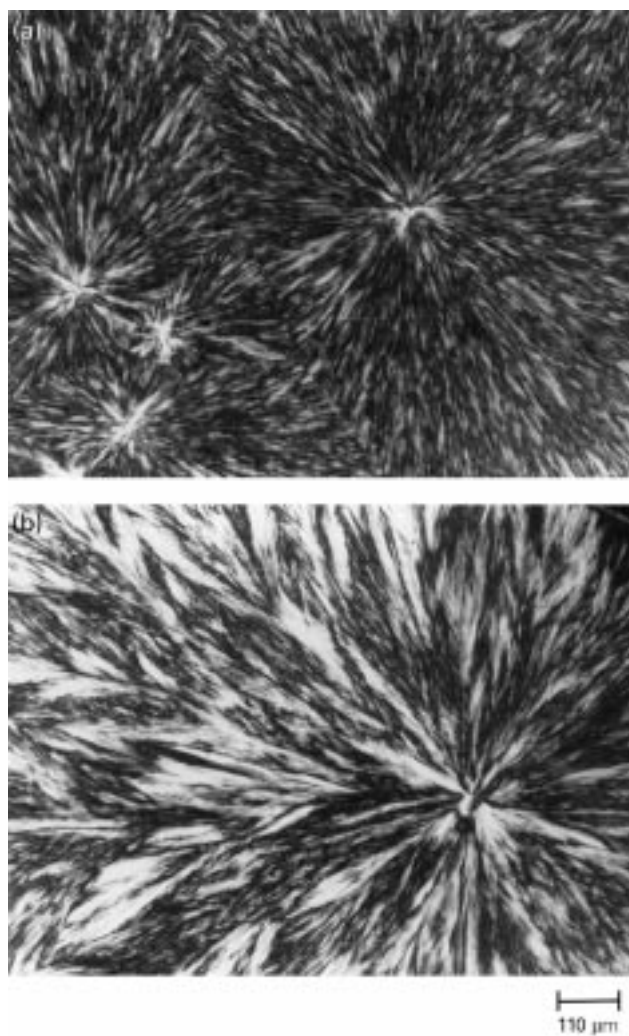


Fig. 6. Optical micrographs of isothermally crystallized samples of iPP/P $\alpha$ P blends at  $T_c = 130^\circ\text{C}$ : (a) 90/10; (b) 70/30 (crossed polars).

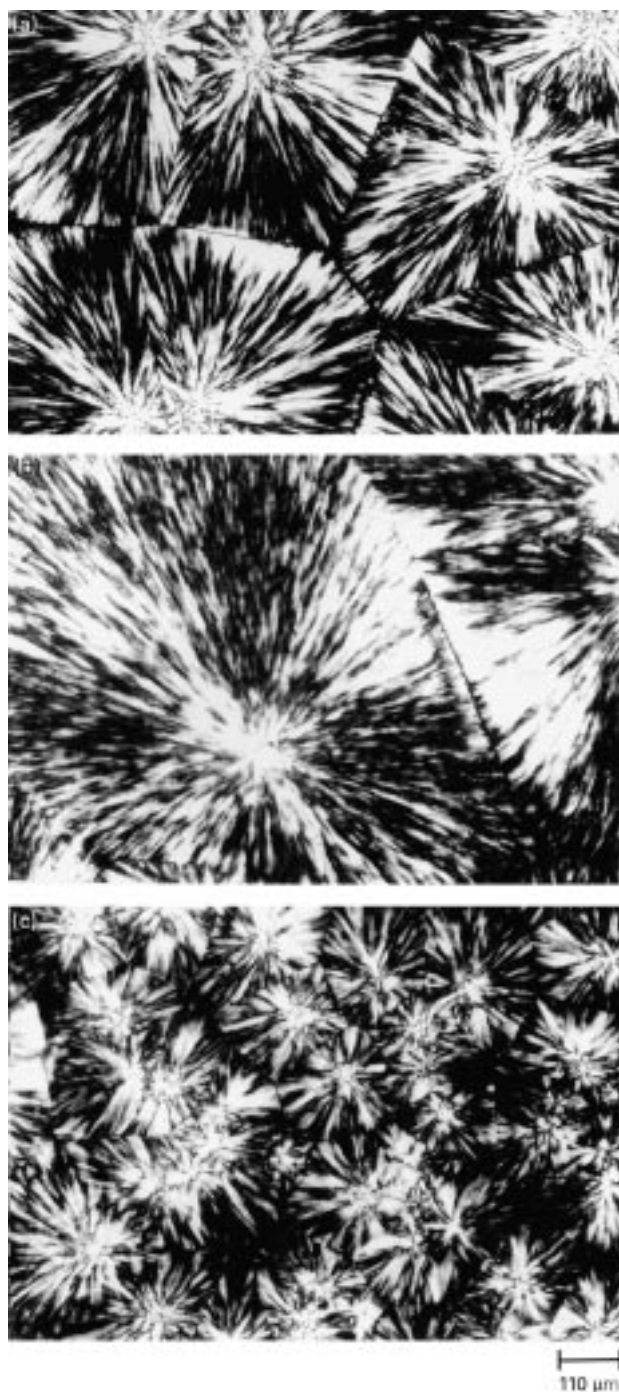


Fig. 7. Optical micrographs of isothermally crystallized samples of iPP/PL blends at  $T_c = 130^\circ\text{C}$ : (a) 90/10; (b) 80/20; (c) 70/30 (crossed polars).

The spherulite radial growth rate in a blend, constituted by a crystallizable and an amorphous component, differs from that of the pure polymer because of the possible interactions between the two components and of the presence of non-crystallizable material that can modify the motions of the macromolecules in the melt. In the case of miscible blends, the presence of the amorphous component

influences the energy relative to both the transport and the nucleation.

For these blends the previous equation is so modified [14–16]:

$$\begin{aligned} \ln G - \ln \varphi_2 + \frac{U^*}{R(T_c - T_\infty)} - \frac{0.2T_m^0 \ln \varphi_2}{\Delta T} \\ = \ln G_0 - \frac{K_g}{T_c \Delta T f} \end{aligned} \quad (2)$$

where  $\varphi_2$  is the volume fraction of the crystallizable component.

In the case of immiscible blends, the presence of the amorphous component can only influence the transport term. In fact, during the crystallization the domains of the non-crystallizable material can be rejected from the growing front of spherulite, and/or occluded and deformed by it.

The presence of these domains, in the melt at the crystallization temperature, can greatly disturb the spherulite growth rate. Energy must be dissipated to occlude and deform the amorphous phase. This energy constitutes a new energetic barrier that can control the spherulites growth in such blends.

The spherulite radial growth rate,  $G$ , as a function of crystallization temperature,  $T_c$ , is reported in Figs. 8 and 9 for the pure polypropylene and iPP/P $\alpha$ P and iPP/PL blends of different composition.

For all the samples the radial growth rate decreases with the crystallization temperature. This result is in agreement with the kinetic theory of crystallization, that expects for crystallizations close to  $T_m$ , a decrease of  $G$  reducing the undercooling.

The addition of the resin to a polypropylene matrix always induces, at a parity of temperature, a spherulite radial growth rate depression that is a function of the composition. Such a depression is very evident at lower crystallization temperatures and vanishes at higher temperatures, confirming that the flow of macromolecules in the melt is the factor that dominates the crystallization process of the iPP/resin system.

At the analyzed crystallization temperatures, the morphological results showed that the polypropylene, for all the iPP/P $\alpha$ P and iPP/PL 95/5 and 90/10 blends, crystallizes in equilibrium with a homogeneous system. The decrease of  $G$  with composition, at a given  $T_c$ , is surely to be ascribed to the diluent effect of the resin. In fact, in agreement with the kinetic theory of crystallization of miscible polymeric blends, the presence of the diluent produces an increase in both the energies relative to the macromolecules transport and to the formation of the nuclei of critical dimension.

For iPP/PL 80/20 and 70/30 blends, the microscopy analysis, conversely, pointed out that in the melt, at  $T_c$ , two phases are present: one rich in polypropylene and the other one in poly(d-limonene). For these blends at  $T_c$ , the iPP, present in the iPP-rich phase, crystallizes enclosing the domains of the PL-rich phase in the interfibrillar spherulite

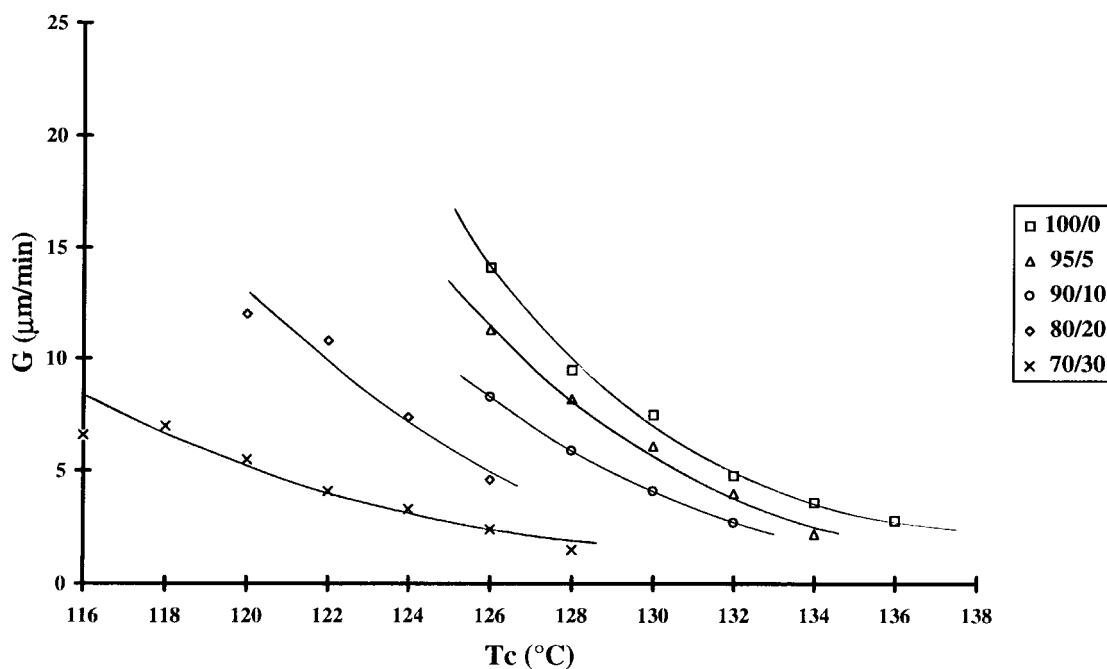


Fig. 8. Spherulite radial growth rate,  $G$ , as a function of crystallization temperature,  $T_c$ , for the iPP/P $\alpha$ P blends.

regions. The decrease of the radial growth rate for these blends is due both to the diluent effect of the resin present in the iPP-rich phase and to the effect that the resin-rich phase domains have on the transport term. In fact, the presence of these domains on the crystallization path, probably produces a further increase in the energy related to the crystallization.

The radial growth rate experimental values of iPP/P $\alpha$ P

blends were analyzed on the basis of Eq. (2) valid for homogeneous blends. Eq. (2) fits well the experimental results. In fact, straight lines were always obtained. From the slopes of such lines it is possible to obtain the  $K_g$  values and therefore the surface free energy of folding ( $\sigma_e$ ).  $\sigma_e$  Values as a function of composition are reported in Table 1.

For the pure polypropylene  $\sigma_e = 189 \text{ erg cm}^{-2}$  [2]. For the blends,  $\sigma_e$  increases with composition. In literature few

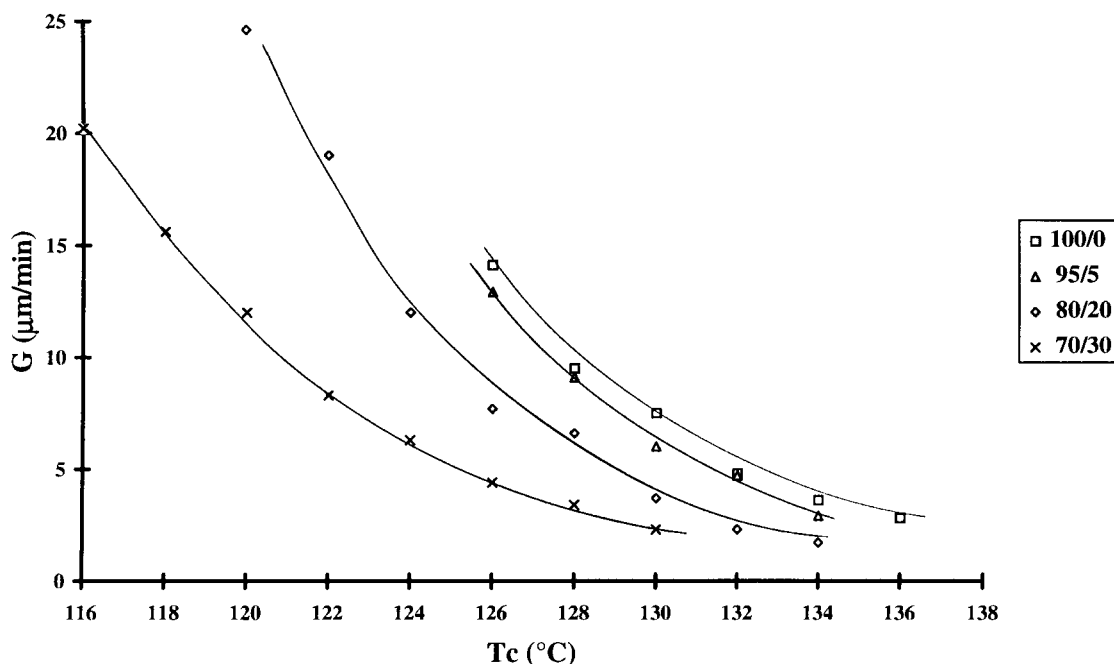


Fig. 9. Spherulite radial growth rate,  $G$ , as a function of crystallization temperature,  $T_c$ , for the iPP/PL blends.

Table 1  
Free energy of folding surface ( $\sigma_e$ ) for iPP/P $\alpha$ P blends

iPP/P $\alpha$ P (wt%)	$\sigma_e$ (erg cm <sup>-2</sup> )
100/0	189
95/5	226
90/10	230
80/20	291
70/30	301

examples report the influences of composition on  $\sigma_e$  in miscible blends, constituted by a crystallizable and an amorphous component [17,18]. In all the cases known by us, a decrease of  $\sigma_e$  is observed with the increase of content of non-crystallizable material. The decrease is sometimes explained supposing that the presence of an amorphous component, influencing the crystallization process, produces an increase of the folding entropy and bears to the formation of crystals with more disordered folding surface. It must be noted, that in all the literature examples, the melt viscosity increases with the increase of amorphous material content.

In our samples, conversely, a decrease of the viscosity is observed with composition, as it will be reported in a forthcoming paper [7]. For the examined blends, the increase of  $\sigma_e$  could indicate a decrease of the entropy of folding and therefore the formation of more homogeneous and regular folding surfaces. The formation of such surfaces is probably in relation to decrease of the melt viscosity in the blend in comparison to that of pure iPP. The iPP chains in blends, having in the melt a lower viscosity, can move easily and probably during crystallization can more regularly fold down.

### 3.2.2. Overall crystallization

The half-time of crystallization as a function of crystallization temperature for different compositions is reported in Figs. 10 and 11 for iPP/P $\alpha$ P and iPP/PL blends respectively.

The addition of resin to iPP, for a given crystallization temperature, always produces an increase in the times required for the overall crystallization process. The entity of such an increase is a function of composition and  $T_c$ : it is large at higher  $T_c$ , whereas it is small at lower crystallization temperatures, in analogy to the results reported for the radial growth rate and confirming the hypothesis according to which, the iPP macromolecules transport is greatly influenced by the presence of the resin.

In order to explain the experimental data it must be considered that at any  $T_c$  the overall crystallization rate depends on nucleation and radial growth rate. At a given  $T_c$ , as already seen, both spherulite growth and nucleation densities decrease increasing the resin content in the blends. The sum of these two effects produces a drastic lowering of the observed overall crystallization rate.

To obtain further information on the crystallization process, the experimental data were analyzed utilizing the theory of phase transformation proposed by Avrami [19]. Kinetics data have been interpreted with the relation suggested by Avrami:

$$1 - X_t = e^{-k t^n} \quad (3)$$

where  $X_t$  is the crystallinity generated at time  $t$ ;  $K$  the overall rate constant;  $n$  the Avrami index, that provides a qualitative indication of the mechanisms of the nucleation processes and crystal growth.

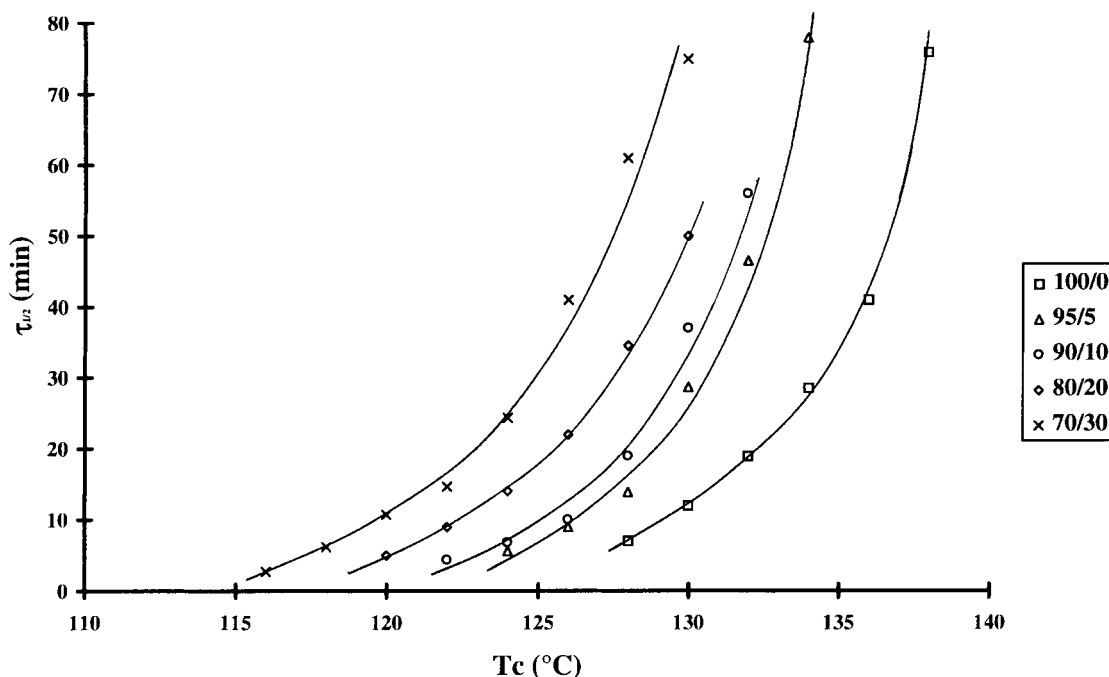


Fig. 10. Half-time of crystallization,  $\tau_{1/2}$ , as a function of crystallization temperature,  $T_c$ , for the iPP/P $\alpha$ P blends.



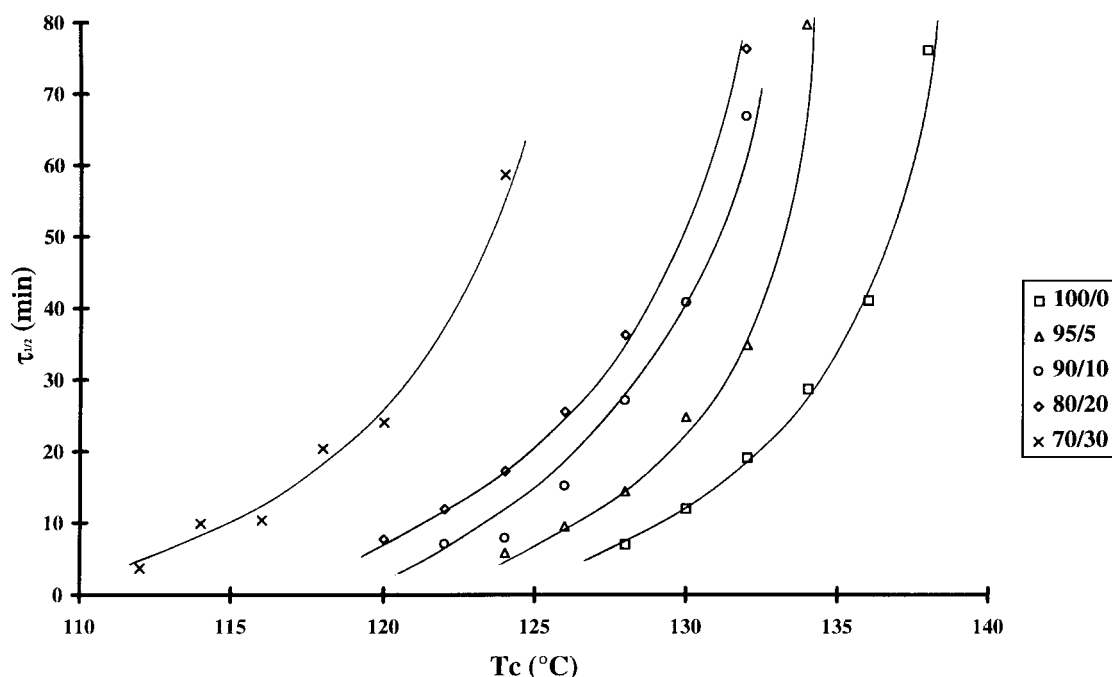


Fig. 11. Half-time of crystallization,  $\tau_{1/2}$ , as a function of crystallization temperature,  $T_c$ , for the iPP/PL blends.

The Avrami equation fits well the experimental results. In fact, reporting  $\log[-\ln(1-X_t)]$  as a function of  $\log t$ , straight lines were always obtained. From the slopes and intercepts of the straight lines it is possible to obtain  $n$  and  $\log K$  values (see Fig. 12). For the pure iPP, independently of the crystallization temperature,  $n$  always has a value of nearly 3, whereas for the blends, for all the compositions and temperatures, the Avrami index is equal to 2. Supposing that the nucleation is heterogeneous for the pure iPP and for the blends, in agreement with the Avrami theory, an  $n = 3$

indicates a tridimensional growth of the crystals, whereas an  $n = 2$  suggests a bidimensional growth. The optical microscopy, showing that the polypropylene always crystallizes assuming a spherulitic morphology, has indicated that the growth of polypropylene crystals is always tridimensional, independently of the presence of resin. Therefore, the Avrami equation is not able to explain the crystallization mechanism in the case of the iPP/resin blends, whereas for the pure polypropylene it is in agreement with the morphological analysis. This probably because the Avrami equation

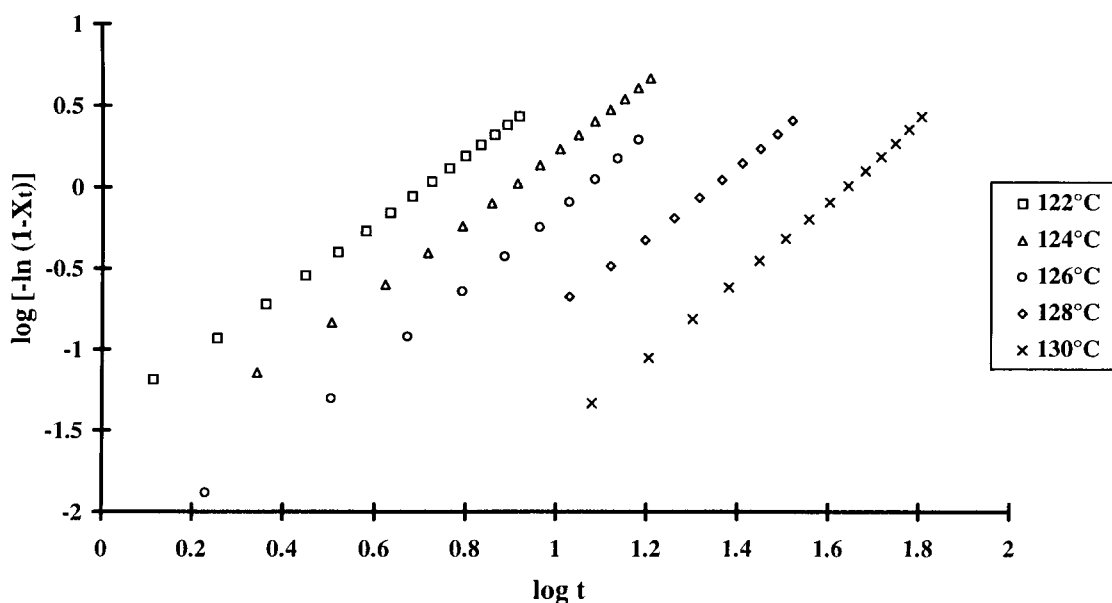


Fig. 12. Trend of  $\log[-\ln(1-X_t)]$  as a function of  $\log t$  for the iPP/PαP 90/10 blend at different crystallization temperatures  $T_c$ .

does not contain terms that consider that during growth the crystallizable molecules have to change their route to englobe, deform and reject the domains of the non-crystallizable component.

This result suggests that the theory of Avrami, just as any theory, must be utilized with caution and confirmed by experimental analysis. In the case of the Avrami equation, applied to blends, an accurate morphological study is therefore necessary.

#### 4. Conclusions

The reported results lead to the following conclusions:

- In the melt at 200°C the iPP constitutes with both the poly( $\alpha$ -pinene) and poly(d-limonene) a homogeneous system. At  $T_c$  the iPP/P $\alpha$ P system is formed by a crystalline iPP phase and a homogeneous amorphous phase. For the iPP/PL system, at  $T_c$ , the phase structure of the amorphous phase is dependent on composition. In the case of iPP/PL 90/10 blends, the amorphous phase is homogeneous, for the 80/20 and 70/30 blends, the amorphous system is composed of two phases: one rich in PL and the other rich in iPP.
- The iPP always crystallizes according to a spherulitic morphology. For the homogeneous blends, at  $T_c$ , a decrease of nucleation density with composition is always observed, consequent on the dilution of the nuclei; on the other hand for the iPP/PL blends that present amorphous phase separation, a relative increase of the nucleation density is observed, indicating that the domains of the rich phase in resin probably behave like nucleating agents.
- The addition of resin always induces, at a parity of  $T_c$ , a diminution of the radial growth rate of spherulites and of overall crystallization rate. For the homogeneous blends, such a decrease is ascribed to the increase of the energy relative to the transport of the macromolecules in the melt and of the energy connected to the formation of nuclei of critical sizes, due to the presence of diluent. For the blends that present phase separation, the decrease of  $G$  is due also to the increase of the transport energy, produced by the presence of domains of the rich phase in resin in the melt at  $T_c$ .

- For the iPP/P $\alpha$ P homogeneous blends, the free energy of folding surface ( $\sigma_e$ ) increases with the composition, indicating that for these blends the folding surfaces are more regular.

#### Acknowledgements

The authors wish to thank Mr Giuseppe Orsello for his useful help in SEM investigations and Mr Loeber of Hercules International Ltd Co. (The Netherlands) for supplying the terpene resins.

#### References

- [1] Pasquini N. *Plast* 1996;2:112.
- [2] Silvis HC. *Trends in Polymer Science* 1997;5:75.
- [3] Marcandalli B, Testa G, Seves A, Martuscelli E. *Polymer* 1991;32:3376.
- [4] Cimmino S, Guarrata P, Martuscelli E, Silvestre C, Buzio PP. *Polymer* 1991;32:3299.
- [5] Cimmino S, Di Pace E, Karasz FE, Martuscelli E, Silvestre C. *Polymer* 1993;34:972.
- [6] Caponetti E, Chillura Martino D, Cimmino S, Floriano MA, Martuscelli E, Silvestre C, Triolo R. *J Mol Structure* 1996;383:75.
- [7] Cimmino S, D'Alma E, Di Lorenzo ML, Di Pace E, Silvestre C. In preparation.
- [8] Cimmino S, D'Alma E, Di Lorenzo ML, Di Pace E, Silvestre C. *J Polym Sci* 1999, in press.
- [9] Lu J, Kamigaito M, Sawamoto M, Higashimura T, Deng Y. *J Appl Polym Sci* 1996;61:1011.
- [10] Vredenburgh W, Foley KF, Scarlatti AN. In: Mark HF, Bikales NM, Overberger CG, Menges GJ, Kroschwitz I, editors. *Encyclopedia of polymer science and engineering*, vol. 14. New York: Wiley, 1988, p. 438.
- [11] Hoffman JD. *Polymer Division, National Bureau of Standards, D.C.* 20234, *SPE Transaction*, 1964.
- [12] Hoffman JD, Davis GT, Lauritzen JI. In: Hannay NB, editor. *Treatise on solid state chemistry*, vol. 3. New York: Plenum Press, 1976:7.
- [13] Hoffman JD. *Polymer* 1982;24:3.
- [14] Boon J, Azcue JM. *J Polym Sci* 1968;6(Part A2):885.
- [15] Martuscelli E. *Polym Eng Sci* 1984;24:563.
- [16] Alfonso GC, Russell TP. *Macromolecules* 1986;19:1143.
- [17] Silvestre C, Cimmino S, Di Pace E. In: Salamone JC, editor. *Crystallizable polymer blends, polymeric materials encyclopedia*, vol. 2. Boca Raton: CRC Press, 1996:1595.
- [18] Cimmino S, Martuscelli E, Silvestre C, Canetti M, De Lalla C, Seves A. *J Polym Sci, Polym Phys Ed* 1989;27:1781.
- [19] Avrami M. *J Chem Phys* 1939;7:1103.